BIOCHEMISTRY
including biophysical chemistry & molecular biology
Article

Biochemistry **2010,** *49,* 5057–5065 5057
DOI: 10.1021/bi1005267

Alanine Scanning Mutagenesis of HIV-1 gp41 Heptad Repeat 1: Insight into the gp120−gp41 Interaction†

Jayita Sen,‡ Tianran Yan,‡ Jizhen Wang,‡ Lijun Rong,§ Lin Tao,‖ and Michael Caffrey*,‡

‡*Department of Biochemistry and Molecular Genetics, University of Illinois, Chicago, Illinois 60607,* §*Department of Microbiology and Immunology, University of Illinois, Chicago, Illinois 60612, and* ‖*Department of Oral Biology, University of Illinois, Chicago, Illinois 60612*

Received April 8, 2010; Revised Manuscript Received May 18, 2010

ABSTRACT: On the basis of mutagenesis, biochemical, and structural studies, heptad repeat 1 of HIV gp41 (HR1) has been shown to play numerous critical roles in HIV entry, including interacting with gp120 in prefusion states and interacting with gp41 heptad repeat 2 (HR2) in the fusion state. Moreover, HR1 is the site of therapeutic intervention by enfuviritide, a peptide analogue of HR2. In this study, the functional importance of each amino acid residue in gp41 HR1 has been systematically examined by alanine scanning mutagenesis, with subsequent characterization of the mutagenic effects on folding (as measured by incorporation into virions), association with gp120, and membrane fusion. The mutational effects on entry can be grouped into three classes: (1) wild type (defined as >40% of wild-type entry), (2) impaired (defined as 5−40% of wild-type entry), and (3) nonfunctional (defined as <5% of wild-type entry). Interestingly, the majority of HR1 mutations (77%) exhibit impaired or nonfunctional entry. Surprisingly, effects of mutations on folding, association, or fusion are not correlated to heptad position; however, folding defects are most often found in the N-terminal region of HR1. Moreover, disruption of the gp41−gp120 interaction is correlated to the C-terminal region of HR1, suggesting that this region interacts most closely with gp120. In summary, the sensitivity of gp41 HR1 to alanine substitutions suggests that even subtle changes in the local environment may severely affect envelope function, thereby strengthening the notion that HR1 is an attractive site for therapeutic intervention.

The HIV[1] and simian immunodeficiency virus envelope proteins are class I fusion proteins synthesized as glycosylated, polyprotein precursors and subsequently cleaved by a cellular furin-like protease into the transmembrane subunit gp41 and the noncovalently associated surface subunit gp120 (*1*−*3*). During entry, gp120 mediates binding to the CD4 and chemokine receptors and gp41 mediates fusion of the viral and target cell membranes (*4*−*6*). HIV and SIV envelope proteins are thought to exist in at least three conformations: (1) preattachment (before receptor engagement), (2) attachment (bound to CD4 and coreceptor), and (3) fusion (in which the viral and target membranes fuse). High-resolution structural information is available for isolated domains in each of the three conformational states. For example, the structure of the SIV gp120 core represents the preattachement state (*7*), and the structure of the HIV gp120 core bound to CD4 domains represents the attachment state (*8*−*10*). Moreover, the structures of the SIV and HIV gp41 ectodomains comprised of highly conserved heptad repeats, termed HR1 and HR2, represent the fusion state (*11*−*15*). However, in each case, significant regions of the gp120−gp41 complex are missing. For example, the gp120 structures characterized to date are missing gp41, and thus, the structures give only limited insight into the conformation of the envelope complex in the preattachment and attachment states.

As alternative approaches, biochemical and mutagenesis studies provide novel insights into envelope structure in various conformations. For example, the potent antiviral enfuviritide (*16*), which is a peptide corresponding to the gp41 HR2 region, interacts with HR1 only after receptor binding, suggesting that HR1 is transiently exposed (*17*, *18*). On the other hand, mutagenesis studies provide insights into the overall architecture of the envelope complex and the importance of individual residues in envelope function. For example, Binley et al. have introduced pairs of non-native cysteines to distant residues of gp120 and gp41 and interpreted the formation of intermolecular disulfide bonds as evidence that these residues are in the proximity of the preattachment conformation (*19*). In other studies, extensive site-directed mutagenesis of the gp120 and gp41 domains has identified long-range intra- and intermolecular interactions and elucidated the importance of specific side chains to membrane fusion (*20*−*32*). In this study, we have analyzed the importance of each amino acid residue of the HIV-1 gp41 HR1 by alanine scanning mutagenesis with the goal of identifying gp41 residues that are important to envelope function, as well as identifying attractive sites for therapeutic intervention.

EXPERIMENTAL PROCEDURES

Mutagenesis and Viral Entry Assays. Mutants were prepared from plasmid pHXB2 (*33*) using the Stratagene QuikChange II site-directed mutagenesis kit with subsequent verification by

†This work was partially supported by National Institutes of Health Grants RO1 AI47674 to M.C. and RO1 AI066709 to L.T. and the Chicago D-CFAR (P30 AI082151).

*To whom correspondence should be addressed. Telephone: (312) 996-4959. Fax: (312) 413-0353. E-mail: caffrey@uic.edu.

[1]Abbreviations: HR, heptad repeat; HIV, human immunodeficiency virus; NMR, nuclear magnetic resonance.

Published on Web 05/19/2010

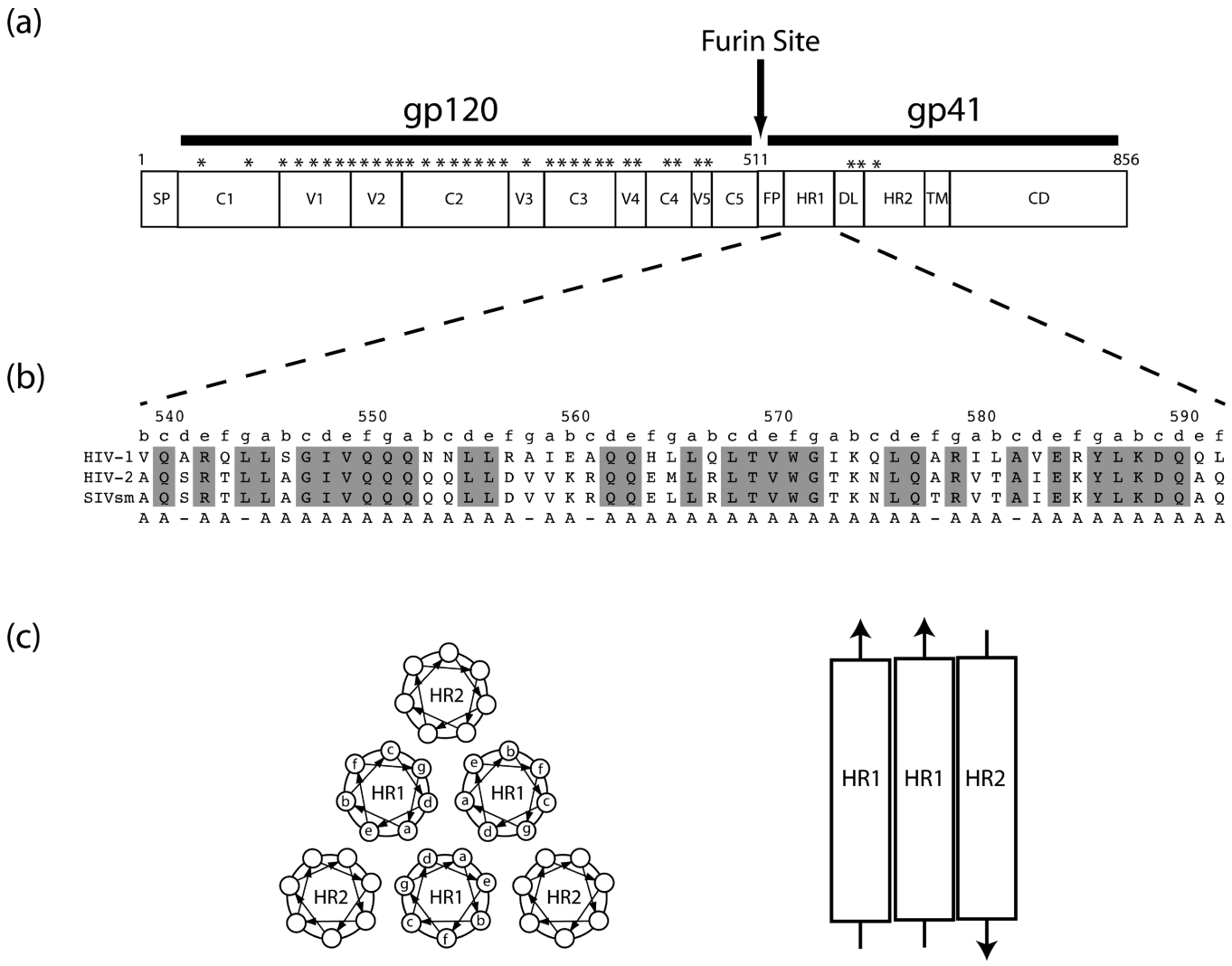

FIGURE 1: (a) Organization of HIV envelope proteins (*36*). Putative glycosylation sites are denoted by asterisks. Domain abbreviations: SP, signal peptide; C1−C5, conserved domains 1−5, respectively; V1−V5, variable domains 1−5, respectively; FP, fusion peptide; DL, disulfide loop; TM, transmembrane domain; CD, cytoplasmic domain. (b) Amino acid sequence alignment of HIV-1, HIV-2, and SIV_{sm} gp41 HR1 (*36*). Conserved residues of gp41 HR1 are highlighted in gray. Residues that are substituted with alanine in this study are denoted below. The numbering corresponds to that of HIV-1 HXB2. Heptad repeat positions are shown as lowercase letters. (c) Schematic diagram of the HR1−HR1 and HR1−HR2 interactions observed in structures of the gp41 fusion state (*11*−*15*).

DNA sequencing. The functionality of gp41 mutants was determined in a luciferase-based entry assay (*34*). For this assay, plasmids pHXB2 (bearing wild-type or mutant gp41) and pNL4-3.Luc.R-E- (*34*) were cotransfected by Lipofectamine 2000 (Invitrogen) into 293T cells, which were maintained in Dulbecco's medium with 10% FBS, 1% L-glutamine, 1% penicillin-streptomycin, and 0.5 mg/mL G418. Forty-eight hours post-transfection, the medium was harvested and filtered through a 0.45 μm filter to make the virus stock. For an assay of viral entry, U87.CD4.CXCR4 cells (*34*), which were maintained in Dulbecco's medium with 15% FBS supplemented with 1 μg/mL puromycin, 300 μg/mL G418, 1% L-glutamine, and 1% penicillin-streptomycin, were seeded to a density of 1×10^5 cells/well of a 12-well cell culture plate in a volume of 1 mL. The following day, 500 μL of the virus stock was added to each of the wells of the U87 cells after removal of the medium. The plates were incubated overnight at 37 °C in a CO_2 incubator. After approximately 16 h, the virus was aspirated and replaced with U87 medium and the cells were allowed to rest for an additional 24 h. Luciferase activity was measured using the Luciferase Assay System from Promega and a Berthold FB12 luminometer running Sirius software. The experiments were conducted in triplicate from transfection to assay of luciferase activity, and thus, the uncertainties represent all stages of the experiment. In all cases, the viral entry levels fell within the linear range of detection [i.e., the values of the wild type and mutants never exceeded 3×10^6 relative light units (*31*)].

p24 Assay. The relative virus concentration of the virus stock was determined by the HIV-1 P24 Antigen Capture Assay Kit (NCI-Frederick Cancer Research and Development Center AIDS Vaccine Program). In this assay, a standard curve was generated by measuring the p24 protein concentration of Triton X-100-lysed HIV-1. Then the p24 concentration of each of the 48 samples was quantified by ELISA, the data of which were fitted to the standard curve.

Western Blot Analysis. Cell lysates were collected from 293T producer cells using lysis buffer [50 mM Tris (pH 7.5), 150 mM NaCl, 5 mM EDTA, 0.5% NP-40, and 0.1% SDS]. The virus pellet was prepared by ultracentrifugation on a cushion of 20% sucrose at 55000 rpm for 35 min using a Beckman SW55Ti rotor. The virus pellets were resuspended in lysis buffer [50 mM Tris (pH 7.5), 150 mM NaCl, 5 mM EDTA, 0.5% NP-40, and 0.1% SDS]. After SDS−PAGE and transfer and after the

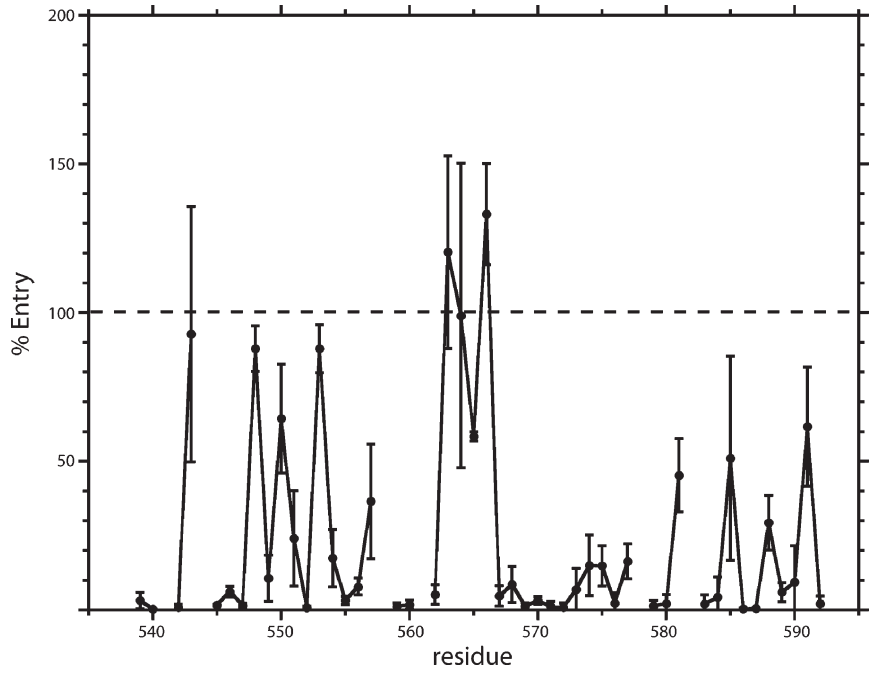

FIGURE 2: Effects of mutations on viral entry with respect to wild-type HIV-1, based on the luciferase reporter assay for entry into U87.CD4.CCR5 cells (cf. Experimental Procedures). The error bars represent the standard deviation of three separate experiments from the transfection step. Entry levels have been normalized to p24 present in virion preparations, as assayed by ELISA.

membranes had been blocked with 5% milk/TBST for gp41 and SuperBlock (Pierce) for gp120, the blots were probed with either goat anti-HIV-1 gp120 polyclonal antibody (United States Biologicals) or mouse anti-HIV-1 gp41 monoclonal antibody [Chessie 8, NIH AIDS Research and Reference Reagent Program (*35*)]. HIV-1 p24 was detected by probing the membrane with mouse anti-HIV-1-p24 antibody (United States Biologicals). The secondary antibody used was peroxidase-conjugated AffiniPure donkey anti-goat or goat anti-mouse IgG (H+L) from Jackson ImmunoResearch Laboratories, Inc., and developed using the ECL kit (Pierce). The relative amount of envelope on the Western blots was determined by a densitometric analysis. Briefly, digital scans of the blots were opened in Photoshop 7.0, and the image was inverted. The appropriate bands were selected with the Lasso function, and the mean intensity and area were measured with the Histogram function. Subsequently, the relative percent was determined by the relationship

$$\text{relative } \% = 100 \times (I_{\text{exp}}A_{\text{exp}} - I_{\text{cont}}A_{\text{cont}})/(I_{\text{wt}}A_{\text{wt}} - I_{\text{cont}}A_{\text{cont}})$$

where I and A denote mean intensity and band area, respectively; the subscripts exp, cont, and wt denote experimental, control (i.e., in the absence of envelope plasmid), and wild type, respectively (*31*). On the basis of analysis of identical samples on different blots, the error is $< 20\%$.

RESULTS

Design of the HIV gp41 HR1 Mutants. As shown in Figure 1a, the gp41 HR1 follows the fusion peptide region of gp41. On the basis of the NMR structure of the ectodomain of SIV gp41 (*14*, *15*), HR1 spans approximately ~54 residues [amino acids 539−592 of HIV-1 strain HXB2 (*36*)]. In this region, 30 residues are conserved among HIV-1, HIV-2, and SIV to give 56% sequence identity [Figure 1b (*36*)]. For reference, the heptad repeat positions (**a**, **b**, **c**, **d**, **e**, **f**, and **g**) are shown above the sequence (*11*). The HR1−HR1 and HR1−HR2 interactions observed in the structures of the gp41 fusion state are shown in Figure 1c (*11*−*15*). Notably, the **a** and **d** positions form the basis of the HR1−HR1 interactions, which are parallel, and the **e** and **g** positions form the basis of the HR1−HR2 interactions, which are antiparallel. In this study, 48 alanine substitutions were generated (five residues were already alanine, and we were unable to generate the L544A mutant). As noted above, gp41 HR1 is the target for therapeutic intervention by enfuviritide, which inhibits HIV-1 but not HIV-2 or SIV (*16*). Interestingly, in the clinical setting, the region encompassing residues 546−556 of HR1 is often the site of resistance to the entry inhibitor enfuviritide (*37*−*39*).

Entry of the Virus for the HIV gp41 HR1 Mutants. The effects of alanine substitutions in gp41 HR1 were first assayed by a luciferase reporter-based viral entry assay, in which viral entry is proportional to the observed luciferase activity (*34*). For comparison to the wild-type envelope, each entry assay has been performed on three separate occasions from the transfection step to the luciferase readout step and normalized to the amount of p24 present in virion preparations. As shown in Figure 2 and summarized in Table 1, the effects of the mutations range from a minimal effect on viral entry (e.g., L566A) to almost complete abolishment (e.g., E560A) relative to the wild-type entry levels. On the basis of the values for entry, the mutants can be divided into three categories as having (1) wild-type entry (defined as $> 40\%$ of wild-type entry), (2) impaired entry (defined as 5−40% of wild-type entry), or (3) nonfunctional entry (defined as $< 5\%$ of wild-type entry). Accordingly, 23% of the mutants exhibit wild-type entry, 31% of the mutants impaired entry, and 46% of the mutants nonfunctional entry.

Mutants that exhibit wild-type entry, defined as exhibiting $> 40\%$ of wild-type entry, include Q543A, I548A, Q550A, N553A, Q563A, H564A, L565A, L566A, L581A, R585A, and L591A. In this group, four of the 11 residues are conserved among the three viral families [I548, Q550, Q563, and L566

Table 1: Summary of HIV-1 gp41 HR1 Alanine Substitutions

	position	% entry	% p24	% gp120	% gp41	phenotype[a]
wild type	−	100	100	100	100	wt
V539A	**b**	3.2	94	< 5	< 5	nf-folding
Q540A	**c**	0.34	89	< 5	< 5	nf-folding
R542A	**e**	0.86	110	< 5	< 5	nf-folding
Q543A	**f**	93	110	210	150	wt
L545A	**a**	1.6	130	86	110	nf-fusion
S546A	**b**	6.1	88	20	16	imp-folding
G547A	**c**	1.5	160	28	31	nf-fusion
I548A	**d**	88	91	130	100	wt
V549A	**e**	11	120	70	76	imp-fusion
Q550A	**f**	64	160	120	150	wt
Q551A	**g**	24	100	170	130	imp-fusion
Q552A	**a**	0.72	200	16	14	nf-folding
N553A	**b**	88	110	130	150	wt
N554A	**c**	17	130	90	130	imp-fusion
L555A	**d**	3.2	110	34	29	nf-fusion
L556A	**e**	7.8	61	14	21	imp-folding
R557A	**f**	37	110	170	120	imp-fusion
I559A	**a**	1.1	140	63	55	nf-fusion
E560A	**b**	1.8	120	< 5	< 5	nf-folding
Q562A	**d**	5.2	97	< 5	< 5	imp-folding
Q563A	**e**	120	100	120	96	wt
H564A	**f**	99	110	160	140	wt
L565A	**g**	58	150	95	160	wt
L566A	**a**	130	76	26	120	wt-association
Q567A	**b**	4.7	120	< 5	11	nf-folding
L568A	**c**	8.6	180	17	110	imp-association
T569A	**d**	1.2	100	< 5	47	nf-association
V570A	**e**	3.2	170	68	130	nf-fusion
W571A	**f**	1.1	160	< 5	41	nf-association
G572A	**g**	0.97	160	< 5	< 5	nf-folding
I573A	**a**	6.9	180	87	180	imp-fusion
K574A	**b**	15	200	100	150	imp-fusion
Q575A	**c**	15	160	54	110	imp-fusion
L576A	**d**	2.3	120	15	68	nf-association
Q577A	**e**	16	130	41	67	imp-fusion
R579A	**g**	1.3	120	42	69	nf-fusion
I580A	**a**	2.1	160	45	98	nf-association
L581A	**b**	45	180	160	180	wt
V583A	**d**	2.0	94	14	55	nf-association
E584A	**e**	4.4	33	< 5	11	nf-folding
R585A	**f**	51	61	55	150	wt-association
Y586A	**g**	0.36	89	11	66	nf-association
L587A	**a**	0.51	150	24	100	nf-association
K588A	**b**	29	55	38	77	imp-association
D589A	**c**	6.0	75	44	64	imp-fusion
Q590A	**d**	9.4	85	16	53	imp-association
Q591A	**e**	62	78	52	100	wt-association
L592A	**f**	2.2	66	7	21	nf-folding

[a]Phenotypes: nf (nonfunctional, defined as < 5% entry), imp (impaired, defined as 5−40% entry), wt (wild type, defined as > 40% entry), folding (defined as < 25% gp41), association (defined as a gp120/gp41 ratio of < 0.5), and fusion (defined as < 40% entry, > 25% gp41, and a gp120/gp41 ratio of > 0.5). Note that wt-association refers to the case of a mutant that exhibits wild-type like entry but weakened gp120−gp41 association.

(Figure 1b)], suggesting that alanine substitution of these residues does not have a significant impact on envelope function. Of the seven remaining mutants in this group, the substituted residues are a mixture of nonconserved hydrophobic residues (L565, L581, and L591) and nonconserved hydrophilic residues (Q543, N553, H564, and R585).

Mutants that exhibit impaired entry, defined as exhibiting 5−40% of wild-type entry, include S546A, V549A, Q551A, N554A, L556A, R557A, Q562A, L568A, I573A, K574A, Q575A, Q577A, L588A, D589A, and Q590A. In this group, 10 of the 15 are well-conserved among the three viral families [V549, Q551, L556, Q562, L568, K574, Q577, K588, D589, and Q590 (Figure 1b)], and thus, the deleterious effects on envelope function are not surprising. On the other hand, the remaining mutants include a nonconserved hydrophobic residue (I573) and nonconserved hydrophilic residues (S546, N554, R557, and Q575), and hence, the impaired entry of the alanine substitutions, particularly in the case of the hydrophilic residues, is somewhat unexpected.

Mutants that exhibit nonfunctional entry, defined as exhibiting < 5% of wild-type entry, include V539A, Q540A, R542A, L545A, G547A, Q552A, L555A, I559A, E560A, Q567A, T569A, V570A, W571A, G572A, L576A, R579A, I580A, V583A, E584A, Y586A, L587A, and L592A. In this group, 15 of the 22 residues are strictly conserved among the three viral families [Q540, R542, L545, G547, Q552, L555, T569, V570, W571, G572, L576, R579, E584, Y586, and L587 (Figure 1b)], and again the deleterious effects of the mutations may be expected. Of the remaining mutants of this category, they are a mixture of nonconserved hydrophobic residues (V539, I559, I580, V583, and L592) and nonconserved hydrophilic residues (E560 and Q567).

Presence of gp120 and gp41 in Mutant Virus. It is next of interest to compare the effects of mutations on viral entry with the amount of gp120 and gp41 present in virion preparations by Western blot analysis as shown in Figure 3 and summarized in Table 1. In addition, the amount of p24 present has been quantified by ELISA (Table 1) and verified by Western blotting. In the case of the wild type, the Western blots clearly show the presence of gp120 and gp41, indicating that envelope protein is incorporated into virus, which includes processing by furin, and that gp120 remains associated with gp41 on the virus surface. We will first consider mutants that exhibit wild-type levels of entry. Not surprisingly, Q543A, I548A, Q550A, N553A, Q563A, H564A, L565A, and L581A exhibit wild-type levels of gp120 and gp41 in virions [defined herein as > 25% gp120 and gp41 with respect to wild-type levels (Figure 3 and Table 1)], suggesting that the mutation has not deleteriously affected incorporation into virions and the stability of the gp120−gp41 complex. Note that the incorporation of the envelope into virions requires surface expression of the envelope, which has been previously shown to be dependent upon proper folding and oligomerization (*40*−*42*), and thus, we will interpret folding on the basis of incorporation of the envelope into virions. Interestingly, L566A, R585A, and Q591A exhibit a significantly decreased level of gp120 with respect to the level of gp41, suggesting that gp120−gp41 association has been weakened (Figure 3 and Table 1). Nonetheless, the entry levels observed for these mutants indicate that their disruption of the gp120−gp41 interaction has only minimal effects on viral entry.

Next we consider the profile of the mutants exhibiting impaired viral entry (S546A, V549A, Q551A, N554A, L556A, R557A, Q562A, L568A, I573A, K574A, Q575A, Q577A, L588A, D589A, and Q590A). Within this category, we observe a number of different profiles in the Western blots. First, S546A, L556A, and Q562A exhibit decreased levels of gp120 and gp41 [defined herein as < 25% of the wild-type level (Figure 3 and Table 1)], which indicates that the envelope proteins are incorporated into virus at significantly lower levels, presumably due to disruption of envelope folding and/or oligomerization (*40*−*42*), and thus, we will designate these mutants as exhibiting defective folding. Second, L568A, K588A, and Q590A exhibit decreased levels of gp120 with respect to the level of gp41 [defined as a gp120/gp41 ratio of < 0.5 (Figure 3 and Table 1)], suggesting

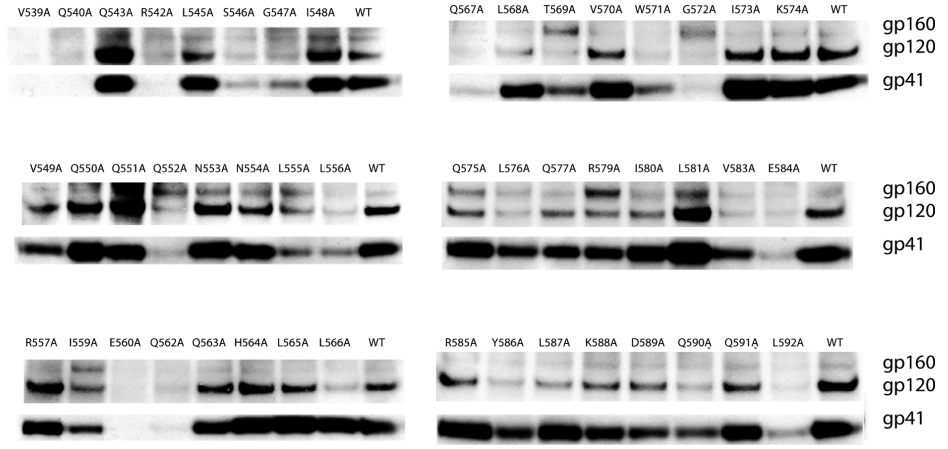

FIGURE 3: Western blot analysis of virion incorporation of envelope and gp120−gp41 association for wild-type HIV-1 and the gp41 HR1 mutants (cf. Experimental Procedures). The positions of gp41, gp120, and gp160 are shown.

that the alanine substitution weakens gp120−gp41 association (i.e., causes shedding). In this case, the disruption of the gp120−gp41 interaction results in impaired entry, and we will designate these mutants as defective in gp120 association. Interestingly, V549A, Q551A, N554A, R557A, I573A, K574A, Q575A, Q577A, and D589A exhibit wild-type levels of gp120 and gp41 in virions (Figure 3 and Table 1). In these cases, the impaired entry is presumably due to disruption of membrane fusion events [the disruption of receptor binding is also possible but seems unlikely in that gp41 HR1 is expected to be distant from the receptor binding sites on gp120 (*10*)], and thus, we will designate this group as being defective in membrane fusion. In summary, the phenotypes of the impaired mutants are divided as follows: 20% defects in folding, 20% defects in gp120 association, and 60% defects in membrane fusion.

Finally, we will consider the expression profile of the mutants exhibiting nonfunctional entry (V539A, Q540A, R542A, L545A, G547A, Q552A, L555A, I559A, E560A, Q567A, T569A, V570A, W571A, G572A, L576A, R579A, I580A, V583A, E584A, Y586A, L587A, and L592A). Mutants V539A, Q540A, R542A, Q552A, E560A, Q567A, G572A, V583A, and L592A exhibit decreased levels of gp120 and gp41, which again indicates that the envelope proteins are not incorporated into virus and thus have resulted in nonfunctional virus. In contrast, mutants T569A, W571A, L576A, I580A, V583A, Y586A, and L587A exhibit decreased levels of gp120 with respect to gp41, which suggests that the mutation has disrupted gp120−gp41 association to a degree that renders the envelope nonfunctional. On the other hand, mutants L545A, G547A, L555A, I559A, V570A, and R579A exhibit wild-type levels of gp120 and gp41 in virions, implicating a defect in membrane fusion. In summary, the phenotypes of the nonfunctional mutants are divided as follows: 41% defects in folding, 32% defects in gp120 association, and 27% defects in membrane fusion.

DISCUSSION

Summary of the gp41 HR1 Mutational Effects. In this study, alanine substitutions at 48 positions within HIV gp41 HR1 have been characterized for effects on viral entry and the profile of envelope present in virions. We have chosen alanine as a substituting residue because of its relatively conservative nature. For example, alanine is found at interior and exterior sites within proteins. Interestingly, we find that the effects on envelope function are not correlated with amino acid type. For example, mutations to 20 hydrophilic and 17 hydrophobic positions exhibited impaired or abrogated entry, supporting the notion that each residue has evolved to serve a purpose, often critical to function. Moreover, even relatively conservative mutations, as evidenced by S546A and T569A, may lead to severe inhibition of viral entry. In total, 77% of the mutants exhibit impaired or abrogated entry. In previous mutagenesis studies performed by our group, we have found impaired or abrogated entry for 57% (12 of 21 residues), 59% (10 of 17 residues), and 50% (13 of 26 residues) of the alanine substitutions within gp120 conserved domain 1 (*32*), gp120 conserved domain 5 (*31*), and the gp41 disulfide loop (*29*), respectively. Taken together, these studies suggest that the HIV envelope is generally sensitive to mutation and further underscores the importance of the gp41 HR1 region to envelope function with respect to other conserved domains. Such an observation may imply that gp41 HR1 is an attractive

Table 2: Summary of HR1 Alanine Substitutions Characterized in Previous Studies

mutant	% entry/fusion	refs
I548A	84[a]	*20*
V549A	100,[b] 80[b]	*24*, *28*
Q551A	100,[b] 60[b]	*24*, *28*
L556A	0,[a] 0,[b] 0,[c] 70[b]	*21*, *22*, *24*, *28*
I559A	0[c]	*21*
Q562A	0[c]	*21*
Q563A	100,[b] 80,[a] 95[b]	*23*, *24*, *28*
L565A	0,[b] 5,[b] 10[b]	*24*, *27*, *28*
L566A	0[c]	*21*
L568A	29,[a] 20,[d] 35[b]	*20*, *25*, *27*
T569A	0[c]	*21*
V570A	0,[b] 0,[d] 0,[a] 4,[b] 25[b]	*23*−*25*, *27*, *28*
W571A	0[d]	*25*
G572A	0,[a] 0,[b] 5[b]	*21*, *22*, *24*, *28*
I573A	0[c]	*21*
K574A	10[d]	*25*
Q577A	100,[b] 30,[a] 100[b]	*23*, *24*, *28*
R579A	0,[b] 30[b]	*24*, *28*
I580A	0[c]	*21*
E584A	0,[a] 3[b]	*20*, *26*
L587A	0[c]	*21*

[a]HXB2 envelope-mediated virus entry. [b]HXB2 envelope-mediated cell−cell fusion. [c]LAI envelope-mediated cell−cell fusion. [d]NL4-3 envelope-mediated virus entry.

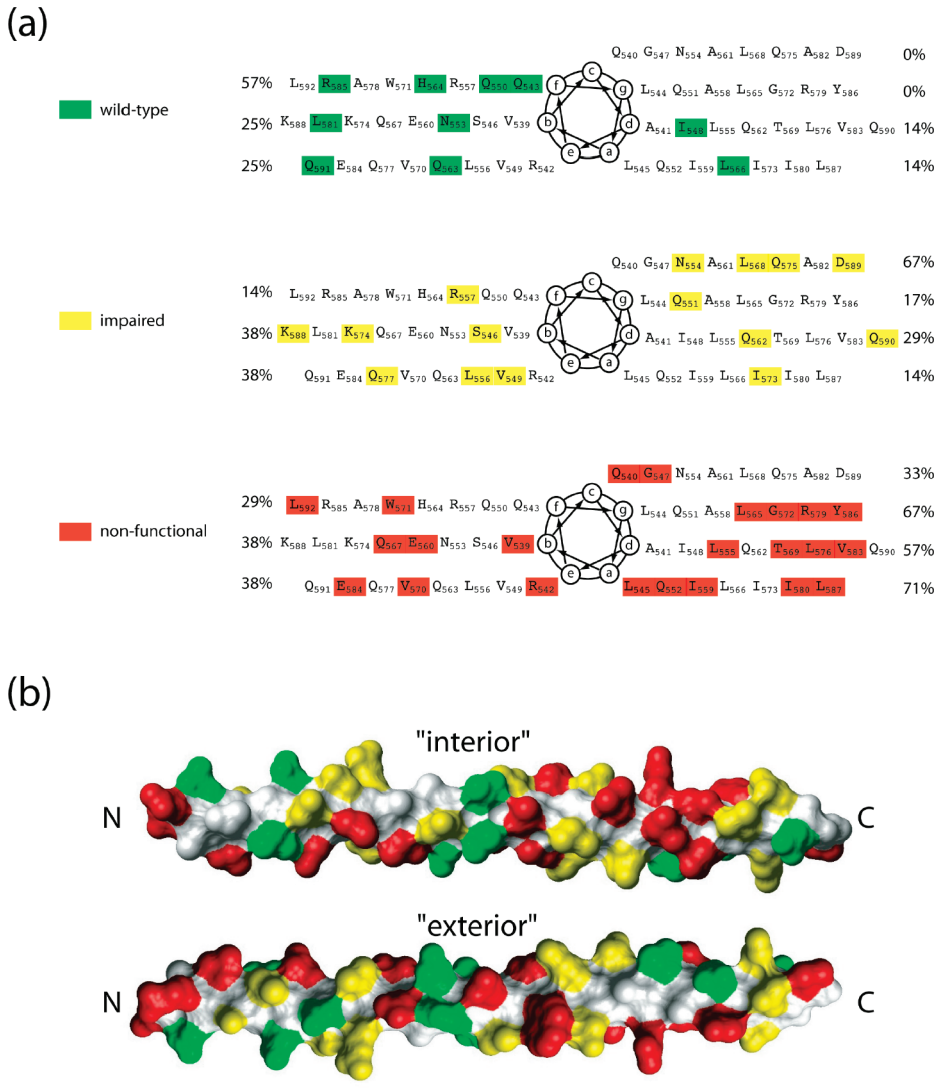

FIGURE 4: Mutational effects of HIV gp41 HR1 on entry with respect to heptad repeat position (a) and location in the HR1 helix (b). In panel a, the relative percentages of entry effects are shown for each position in the heptad repeat. The structure of HR1 is taken from that present in the HIV gp41 fusion state (*10*−*15*) and presented in a space filling representation. The interior face corresponds to positions **a** and **d** (i.e., those that interact with another HR1 in the fusion state); the exterior face corresponds to positions **b** and **f** (i.e., those that that are solvent-exposed in the fusion state).

target for therapeutics. Indeed, this notion is strongly supported by the clinical success of enfuviritide, which targets gp41 HR1 (*16*). As noted above, mutations within the sequence of residues 546−556 are often correlated with resistance to enfuviritide (*37*). Furthermore, Wexler-Cohen and Shai have shown that the 25 N-terminal residues of enfuviritide, which are expected to directly interact with the N-terminal region of gp41 HR1, are most important to the peptide's antiviral activity (*43*). Interestingly, the V549A mutation is the most frequent mutation correlated with enfuviritide resistance (*38*, *39*). With respect to our study, we found that the V549A mutation exhibits a reduced level of entry (11% of the wild-type leve) and a phenotype of reduced membrane fusion (Table 1). Consequently, in the clinical setting, this mutation would be interpreted as a compromise between significantly reduced viral fitness and increased resistance to enfuviritide, with the increased resistance due to the removal of intermolecular hydrophobic contacts between V549 and the enfuviritide peptide (*39*).

Previous Mutagenesis Studies of gp41 HR1. It is next of interest to compare the results presented here to the results of previous mutagenesis studies of gp41 HR1. In Table 2, we summarize envelope function of previously characterized alanine substitutions of HIV-1 gp41 HR1. Note that previous studies have targeted specific positions (e.g., heptad repeat positions **a** and **d**); in contrast, this study represents the first comprehensive mutagenesis study of gp41 HR1. In the previous mutagenesis studies, envelope function was measured by a pseudotyping assay, which is analogous to the assay used in this work and some other studies (*20*, *22*, *23*, *25*); alternatively, envelope function was assayed by a cell−cell fusion assay in which viral envelope proteins are expressed in one cell line and mixed with cells expressing CD4 and coreceptor (*21*, *24*, *26*−*28*). In total, previous studies have characterized alanine substitutions at 21 of the 48 positions examined in this work. In cases where multiple groups studied the identical mutant, the studies are in general agreement. However, note that Q577A has been reported to exhibit both wild-type function (*24*) and impaired function (*23*) by different groups. The differences are most likely due to different assays of envelope function (virus entry vs cell−cell fusion). With respect to the set of mutations presented here, the observed wild-type functions of I548A, Q563A, and Q577A (Table 1) are in close agreement with that reported previously

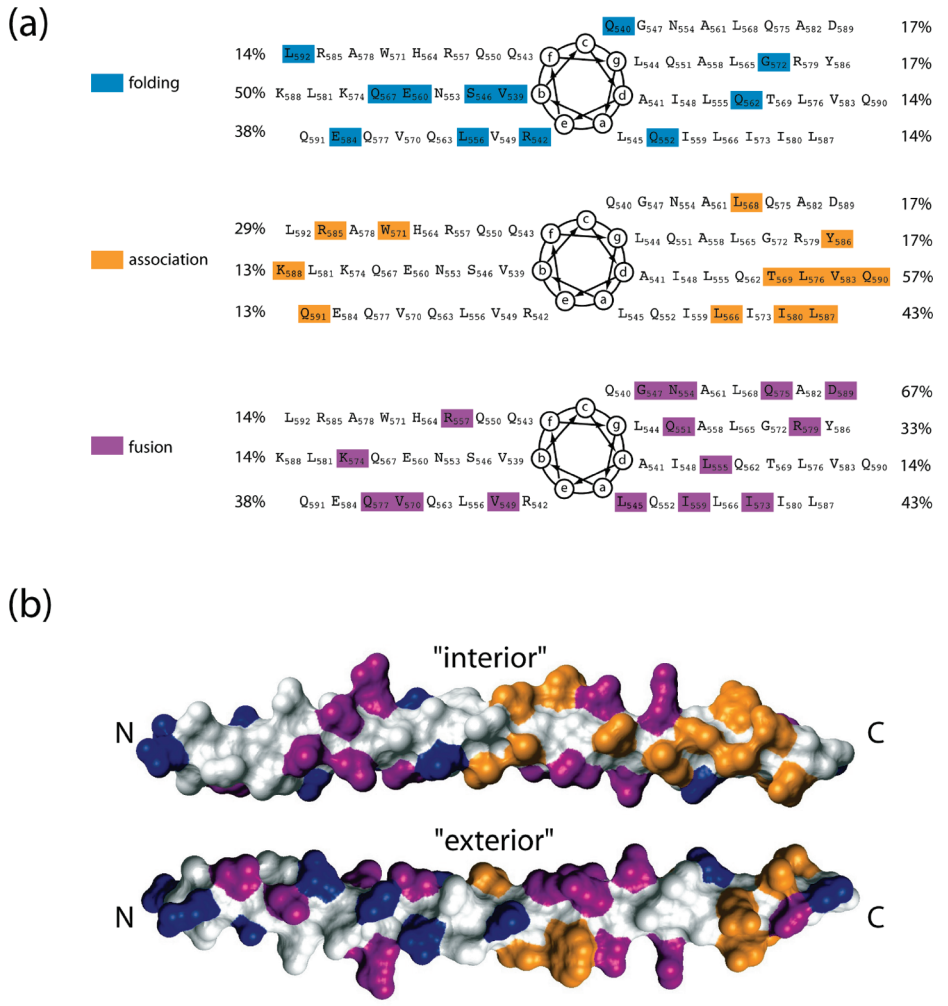

FIGURE 5: Mutational effects of HIV gp41 HR1 on phenotype with respect to heptad repeat position (a) and location in the HR1 helix (b). In panel a, the relative percentages of phenotype effects are shown for each position in the heptad repeat. (b) The structure of HR1 is taken from that in the HIV gp41 fusion state (*10*−*15*) and presented in a space filling representation. The interior face corresponds to positions **a** and **d** (i.e., those that interact with another HR1 in the fusion state); the exterior face corresponds to positions **b** and **f** (i.e., those that that are solvent-exposed in the fusion state).

(Table 2). Moreover, the impaired function or nonfunction observed for L556A, I559A, Q562A, L568A, T569A, V570A, W571A, G572A, I573A, K574A, R579A, I580A, E584A, and L587A (Table 1) are also in close agreement with that reported previously (Table 2). On the other hand, our results for V549A, Q551A, L565A, and L566A are in contrast to those of previous studies (Tables 1 and 2), which is again presumably due to different assays of envelope function (i.e., virus entry in our case vs cell−cell fusion in the previous studies). Finally, we note that 27 of the mutations characterized in this study are novel.

Location of the Mutations in gp41 HR1. It is interesting to consider the position of the mutated residues with respect to the heptad repeat position and known structures of gp41 HR1. In Figure 4, we have color-coded the mutational effects on entry with respect to position in the helical wheel and high-resolution structure of gp41 HR1 in the fusion state (*11*−*15*). As discussed above, gp41 HR1 is thought to be a homotrimer in all conformational states, and on the basis of the fusion structures, the HR1−HR1 contacts are primarily at the **a** and **d** sites (Figure 1c and refs (*11*−*15*)). Moreover, in the fusion sate, the HR1−HR2 contacts are primarily at the **e** and **g** sites of HR1, and the **b** and **f** sites of HR1 are solvent-exposed (Figure 1c and refs (*11*−*15*)). Consequently, the **b**, **e**, **f**, and **g** sites would be expected to be available for interactions with gp120 domains, as well as with other gp41 domains, in the prefusion conformations. As shown in Figure 4a, we observe impaired or nonfunctional mutants at all positions in the heptad repeat; the least disruptive site is at position **f**, and the most disruptive sites are at positions **a**, **c**, **d**, and **g**. As shown in Figure 4b, the effects on entry are evenly dispersed along the sequence (in this figure, the "interior" represents the **a** and **d** face of HR1 and the "exterior" represents the **b** and **f** face of HR1). One interpretation is that essentially all heptad positions in HR1, with the exception of the **f** sites, are involved in interactions with either gp41 domains (e.g., fusion peptide, disulfide loop, or HR2) or gp120 domains via direct or indirect propagated effects. Alternatively, one could interpret the lack of correlation between entry effects and heptad repeat position as evidence that the heptad repeat does not exist for the pre-attachment and/or attachment conformations of the envelope.

In Figure 5, we have color-coded the mutational effects on phenotype to the position in the helical wheel and high-resolution structure of gp41 HR1 in the fusion state. With respect to incorporation of envelope into virus, which has previously been suggested to be correlated with envelope folding and oligomerization (*40*−*42*), mutational effects are not well-correlated to heptad position (Table 1 and Figure 5a), although positions **b** and

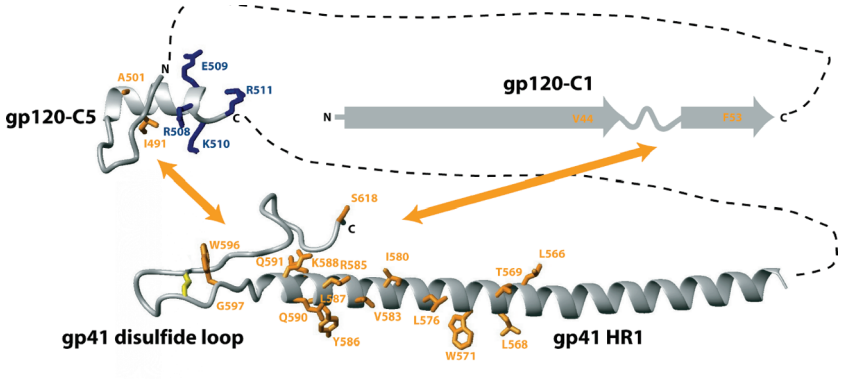

FIGURE 6: Mutagenesis-based model for long-range intermolecular interactions between gp120 and gp41. The orange residues represent alanine substitutions that disrupt association of gp120 with gp41. For reference, the furin processing site is colored blue. The structure of gp120 C1 was based on secondary structure predictions (*32*); the structure of gp120 C5 was taken from Guilhaudis et al. (*47*), and the structures of gp41 HR1 and the disulfide loop were taken from Caffrey et al. (*14*, *15*).

e appear to be most sensitive to mutation. Interestingly, the majority of the mutants exhibiting a defective folding phenotype are found in the N-terminal region of HR1 (Table 1 and Figure 5b), suggesting that this region plays critical roles in envelope folding. With respect to mutants exhibiting putative defects in membrane fusion, the **b** and **f** sites are least sensitive and the **a**, **d**, **e**, and **g** sites are most sensitive (Figure 5a). Moreover, the fusion phenotype is distributed throughout the HR1 sequence (Figure 5b). Together, these observations are consistent with the long-range contacts of HR1 found in the fusion state (refs (*11*−*15*) and Figure 1c). Recently, Markosyan et al. directly measured the fusion properties of alanine substitutions at the **e** and **g** heptad sites within HR1 and found that the most important effects on fusion occurred in the C-terminal region of HR1 (*28*), which would seem to be at odds with our results. However, the entry effects presented herein for the **e** and **g** sites of HR1 are in close agreement with those of Markosyan et al. [with the exception of L556A, which may be attributed to different assays of function (cf. Table 2)]. In our study, other sites in the N-terminal region of HR1 (e.g., L545A, G547A, and V549A) exhibit putative defects in membrane fusion (with the caveat that we have not directly measured fusion and thus the phenotype could be due to disruption of receptor binding or an unknown intermediate step). Consequently, our interpretation is that the effects of the **e** and **g** sites on fusion are due to direct interactions with HR2, as proposed previously (*28*), and the effects at other sites are due to indirect effects.

It is next of interest to consider the location of the mutants that exhibit increased level of dissociation of gp120 (Table 1). Previously, alanine scanning mutagenesis has been exploited to identify "hot spots" of protein−protein interactions (*44*−*46*), which is relevant in this study of gp120−gp41 interactions for which there is no high-resolution structural information. As shown in Figure 5a, mutations to the **a** and **d** sites are most disruptive. Interestingly, mutants that disrupt gp120 association are generally found in the C-terminal region of HR1, which implies that this region has its strongest interaction with gp120 in the preattachment state, and thus, this region of HR1 is a hot spot. Notably, Cao et al. have previously observed weakened gp120 association for mutations in the N-terminal region, S528T, M530S, Q552L, L555G, and Q562L, as well as mutations in the C-terminal region, E584A and V608A (*20*).

Previously, two domains of gp120, conserved domains 1 and 5, and one other domain of gp41, the disulfide loop, have been subjected to comprehensive mutagenesis (*29*, *31*, *32*). In Figure 6, we have modeled long-range interactions between gp120 and gp41 based on mutagenic effects on gp120−gp41 association. In this figure, the structures of gp120 conserved domains 1 and 5, which are largely absent from available crystal structures, are based on the predicted secondary structure and solution structure, respectively (*32*, *47*). The structures of gp41 HR1 and the disulfide loop are based on the solution structure in the fusion state (*14*, *15*). Mutation sites found to be most disruptive to gp120−gp41 association are colored orange. For reference, the border between gp120 and gp41, the furin recognition site, is colored blue, and putative long-range intermolecular interactions are denoted by orange arrows. We note that arginine, isoleucine, tryptophan, and tyrosine are the four most common amino acids found at hot spots of protein interfaces in general (*44*−*46*), which is consistent with the observed association defects of mutant I491A in gp120 conserved domain 5 (*31*) and mutants W571A, I580A, R585A, and Y586A in gp41 HR1. Interestingly, in our previous alanine scanning mutagenesis study of the gp41 disulfide loop (*29*), we found that mutants W596A and G597A, residues that are close to the C-terminal region of HR1, were most disruptive to the gp120−gp41 interaction, thereby supporting the notion that the C-terminal region of HR1 is the site of interaction with gp120. In summary, the alanine scanning mutagenesis studies give new insights into the gp120−gp41 interaction, an interaction that has been intractable to high-resolution structural studies to date. Studies that aim to better characterize the gp120−gp41 interaction site by a combination of mutagenesis, biochemistry, and structural biology techniques are currently underway in our laboratories.

ACKNOWLEDGMENT

Reagents pNL4-3.Luc.R-E-, U87.CD4.CCR5, and HIV-1 gp41 Hybridoma (Chessie 8) were obtained through the NIH AIDS Research and Reference Program.

REFERENCES

1. Freed, E., and Martin, M. (1995) The role of human immunodeficiency virus type 1 envelope glycoproteins in virus infection. *J. Biol. Chem. 270*, 23833–23836.
2. McCune, J. M., Rabin, L. B., Feinberg, M. B., Lieberman, M., Kosek, J. C., Reyes, G. R., and Weissman, I. L. (1988) Endoproteolytic cleavage of gp160 is required for the activation of human immunodeficiency virus. *Cell 53*, 55–67.

3. Moulard, M., Hallenberger, S., Garten, W., and Klenk, H. (1999) Processing and routage of HIV glycoproteins by furin to the cell surface. *Virus Res. 60*, 55–65.
4. Gallo, S., Finnegan, C., Viard, M., Raviv, Y., Dimitrov, A., Rawat, S., Puri, A., Durrell, S., and Blumenthal, R. (2003) The HIV Env-mediated fusion reaction. *Biochim. Biophys. Acta 1614*, 36–50.
5. Bazan, H., Alkhatib, G., Broder, C., and Berger, E. (1998) Patterns of CCR5, CXCR4, and CCR3 usage by envelope glycoproteins from human immunodeficiency virus type 1 primary isolates. *J. Virol. 72*, 4485–4491.
6. Björndal, A., Deng, H., Jansson, M., Fiore, J. R., Colognesi, C., Karlsson, A., Albert, J., Scarlatti, G., Littman, D. R., and Fenyo, E. M. (1997) Coreceptor usage of primary human immunodeficiency virus type 1 isolates varies according to biological phenotype. *J. Virol. 71*, 7478–7487.
7. Chen, B., Vogan, E., Gong, H., Skehel, J., Wiley, D., and Harrison, S. (2005) Structure of an unliganded simian immunodeficiency virus gp120 core. *Nature 433*, 834–841.
8. Kwong, P., Wyatt, R., Robinson, T., Sweet, R., Sodroski, J., and Hendrickson, W. (1998) Structure of an HIV gp120 envelope glycoprotein in complex with the CD4 receptor and a neutralizing human antibody. *Nature 393*, 648–659.
9. Huang, C., Tang, M., Zhang, M., Majeed, S., Montabana, E., Stanfield, R., Dimitrov, D., Korber, B., Sodroski, J., and Wilson, I. (2005) Structure of a V3-containing HIV-1 gp120 core. *Science 310*, 1025–1028.
10. Pancera, M., Majeed, S., Ban, Y. E., Chen, L., Huang, C. C., Kong, L., Kwon, Y. D., Stuckey, J., Zhou, T., Robinson, J. E., Schief, W. R., Sodroski, J., Wyatt, R., and Kwong, P. D. (2010) Structure of HIV-1 gp120 with gp41-interactive region reveals layered envelope architecture and basis of conformational mobility. *Proc. Natl. Acad. Sci. U.S.A. 107*, 1166–1171.
11. Chan, D., Fass, D., Berger, J., and Kim, P. (1997) Core structure of gp41 from the HIV envelope glycoprotein. *Cell 89*, 263–273.
12. Weissenhorn, W., Dessen, A., Harrison, S., Skehel, J., and Wiley, D. (1997) Atomic structure of the ectodomain from HIV-1 gp41. *Nature 387*, 426–430.
13. Tan, K., Liu, J.-H., Wang, J.-H., Shen, S., and Lu, M. (1997) Atomic structure of a thermostable subdomain of HIV-1 gp41. *Proc. Natl. Acad. Sci. U.S.A. 94*, 12203–12308.
14. Caffrey, M., Cai, M., Kaufman, J., Stahl, S., Wingfield, P., Covell, D., Gronenborn, A., and Clore, G. (1998) Three-dimensional solution structure of the 44 kDa ectodomain of SIV gp41. *EMBO J. 17*, 4572–4584.
15. Caffrey, M. (2001) Model for the structure of the HIV gp41 ectodomain: Insight into the intermolecular interactions of the gp41 loop. *Biochim. Biophys. Acta 1536*, 116–122.
16. Matthews, T., Salgo, M., Greenberg, M., Chung, J., DeMasi, R., and Bolognesi, D. (2004) Enfuvirtide: The first therapy to inhibit the entry of HIV-1 into host CD4 lymphocytes. *Nat. Rev. Drug Discovery 3*, 215–225.
17. Mkrtchyan, S. R., Markosyan, R. M., Eadon, M. T., Moore, J. P., Melikyan, G. B., and Cohen, F. S. (2005) Ternary complex formation of human immunodeficiency virus type 1 Env, CD4, and chemokine receptor captured as an intermediate of membrane fusion. *J. Virol. 79*, 11161–1169.
18. Melikyan, G. B., Egelhofer, M., and von Laer, D. (2006) Membrane-anchored inhibitory peptides capture human immunodeficiency virus type 1 gp41 conformations that engage the target membrane prior to fusion. *J. Virol. 80*, 3249–3258.
19. Binley, J., Sanders, R., Clas, B., Schuelke, N., Master, A., Guo, Y., Kajumo, F., Anselma, J., Maddon, P., Olson, W., and Moore, J. (2000) A recombinant human immunodeficiency virus type 1 envelope glycoprotein complex stabilized by an intermolecular disulfide bond between the gp120 and gp41 subunits is an antigenic mimic of the trimeric virion-associated structure. *J. Virol. 74*, 627–643.
20. Cao, J., Bergeron, L., Helseth, E., Thali, M., Repke, H., and Sodroski, J. (1993) Effects of amino acid changes in the extracellular domain of the human immunodeficiency virus type 1 gp41 envelope glycoprotein. *J. Virol. 67*, 2747–2755.
21. Poumbourios, P., Wilson, K. A., Center, R. J., El Ahmar, W., and Kemp, B. E. (1997) Human immunodeficiency virus type 1 envelope glycoprotein oligomerization requires the gp41 amphipathic α-helical/leucine zipper-like sequence. *J. Virol. 71*, 2041–2049.
22. Weng, Y., and Weiss, C. D. (1998) Mutational analysis of residues in the coiled-coil domain of human immunodeficiency virus type 1 transmembrane protein gp41. *J. Virol. 72*, 9676–9682.
23. Weng, Y., Yang, Z., and Weiss, C. D. (2000) Structure-function studies of the self-assembly domain of the human immunodeficiency virus type 1 transmembrane protein gp41. *J. Virol. 74*, 5368–5372.
24. Lu, M., Stoller, M. O., Wang, S., Liu, J., Fagan, M. B., and Nunberg, J. H. (2001) Structural and functional analysis of interhelical interactions in the human immunodeficiency virus type 1 gp41 envelope glycoprotein by alanine-scanning mutagenesis. *J. Virol. 75*, 11146–11156.
25. Mo, H., Konstantinidis, A. K., Stewart, K. D., Dekhtyar, T., Ng, T., Swift, K., Matayoshi, E. D., Kati, W., Kohlbrenner, W., and Molla, A. (2004) Conserved residues in the coiled-coil pocket of human immunodeficiency virus type 1 gp41 are essential for viral replication and interhelical interaction. *Virology 329*, 319–327.
26. York, J., and Nunberg, J. H. (2004) Role of hydrophobic residues in the central ectodomain of gp41 in maintaining the association between human immunodeficiency virus type 1 envelope glycoprotein subunits gp120 and gp41. *J. Virol. 78*, 4921–4926.
27. Suntoke, T. R., and Chan, D. C. (2005) The fusion activity of HIV-1 gp41 depends on interhelical interactions. *J. Biol. Chem. 280*, 19852–19857.
28. Markosyan, R. M., Leung, M. Y., and Cohen, F. S. (2009) The six-helix bundle of human immunodeficiency virus Env controls pore formation and enlargement and is initiated at residues proximal to the hairpin turn. *J. Virol. 83*, 10048–10057.
29. Jacobs, A., Sen, J., Rong, L., and Caffrey, M. (2005) Alanine scanning mutants of the HIV gp41 loop. *J. Biol. Chem. 280*, 27284–27288.
30. Sen, J., Jacobs, A., Jiang, H., Rong, L., and Caffrey, M. (2007) The disulfide loop of gp41 is critical to the furin recognition site of HIV gp160. *Protein Sci. 16*, 1236–1241.
31. Sen, J., Jacobs, A., and Caffrey, M. (2008) Role of the HIV gp120 conserved domain 5 in processing and viral entry. *Biochemistry 47*, 7788–7795.
32. Wang, J., Sen, J., Rong, L., and Caffrey, M. (2008) Role of the HIV gp120 conserved domain 1 in processing and viral entry. *J. Biol. Chem. 283*, 32644–32649.
33. Page, K., Landau, N., and Littman, D. (1990) Construction and use of a human immunodeficiency virus vector for analysis of virus infectivity. *J. Virol. 64*, 5270–5276.
34. Connor, R., Chen, B., Choe, S., and Landau, N. (1995) Vpr is required for efficient replication of human immunodeficiency virus type-1 in mononuclear phagocytes. *Virology 206*, 935–944.
35. Abacioglu, Y. H., Fouts, T. R., Laman, J. D., Claassen, E., Pincus, S. H., Moore, J. P., Roby, C. A., Kamin-Lewis, R., and Lewis, G. K. (1994) Epitope mapping and topology of baculovirus-expressed HIV-1 gp160 determined with a panel of murine monoclonal antibodies. *AIDS Res. Hum. Retroviruses 10*, 371–381.
36. Douglas, N., Munro, G., and Daniels, R. (1997) HIV/SIV glycoproteins: Structure-function relationships. *J. Mol. Biol. 273*, 122–149.
37. Sista, P. R., Melby, T., Davison, D., Jin, L., Mosier, S., Mink, M., Nelson, E. L., DeMasi, R., Cammack, N., Salgo, M. P., Matthews, T. J., and Greenberg, M. L. (2004) Characterization of determinants of genotypic and phenotypic resistance to enfuvirtide in baseline and on-treatment HIV-1 isolates. *AIDS 18*, 1787–1794.
38. Covens, K., Kabeya, K., Schrooten, Y., Dekeersmaeker, N., Van Wijngaerden, E., Vandamme, A. M., De Wit, S., and Van Laethem, K. (2009) Evolution of genotypic resistance to enfuvirtide in HIV-1 isolates from different group M subtypes. *J. Clin. Virol. 44*, 325–328.
39. Eggink, D., Langedijk, J. P., Bonvin, A. M., Deng, Y., Lu, M., Berkhout, B., and Sanders, R. W. (2009) Detailed mechanistic insights into HIV-1 sensitivity to three generations of fusion inhibitors. *J. Biol. Chem. 284*, 26941–26950.
40. Bird, C., Gleeson, P., and McCluskey, J. (1990) Expression of human immunodeficiency virus 1 (HIV-1) envelope gene products transcribed from a heterologous promoter. Kinetics of HIV-1 envelope processing in transfected cells. *J. Biol. Chem. 265*, 19151–19157.
41. Otteken, A., Earl, P. L., and Moss, B. (1996) Folding, assembly, and intracellular trafficking of the human immunodeficiency virus type 1 envelope glycoprotein analyzed with monoclonal antibodies recognizing maturational intermediates. *J. Virol. 70*, 3407–3415.
42. Ellgaard, L., and Helenius, A. (2003) Quality control in the endoplasmic reticulum. *Nat. Rev. Mol. Cell Biol. 4*, 181–191.
43. Wexler-Cohen, Y., and Shai, Y. (2007) Demonstrating the C-terminal boundary of the HIV 1 fusion conformation in a dynamic ongoing fusion process and implication for fusion inhibition. *FASEB J. 21*, 3677–3684.
44. DeLano, W. L. (2002) Unraveling hot spots in binding interfaces: Progress and challenges. *Curr. Opin. Struct. Biol. 12*, 14–20.
45. Moreira, I. S., Fernandes, P. A., and Ramos, M. J. (2007) Hot spots: A review of the protein-protein interface determinant amino-acid residues. *Proteins 68*, 803–812.
46. Bogan, A. A., and Thorn, K. S. (1998) Anatomy of hot spots in protein interfaces. *J. Mol. Biol. 280*, 1–9.
47. Guilhaudis, L., Jacobs, A., and Caffrey, M. (2002) Solution structure of the HIV gp120 C5 domain. *Eur. J. Biochem. 269*, 4860–4867.